Diagnostic Accuracy of Lung Ultrasound for Pulmonary Tuberculosis in out-patients from Papua New Guinea, a Resource-Limited setting

Maria Lightowler , Juno Min , Anna Nape , Thelma Galowa , Carolyn Hemo , Erin Stratta , Matthew Fentress , Stefan Weber , Mischa Huson , Laura Sannino , Sarala Nicholas , Helena Huerga

PII: S1201-9712(25)00461-8
DOI: https://doi.org/10.1016/j.ijid.2025.108239
Reference: IJID 108239

To appear in: *International Journal of Infectious Diseases*

Received date: 1 October 2025
Revised date: 14 November 2025
Accepted date: 18 November 2025

Please cite this article as: Maria Lightowler , Juno Min , Anna Nape , Thelma Galowa , Carolyn Hemo , Erin Stratta , Matthew Fentress , Stefan Weber , Mischa Huson , Laura Sannino , Sarala Nicholas , Helena Huerga , Diagnostic Accuracy of Lung Ultrasound for Pulmonary Tuberculosis in out-patients from Papua New Guinea, a Resource-Limited setting, *International Journal of Infectious Diseases* (2025), doi: https://doi.org/10.1016/j.ijid.2025.108239

Diagnostic Accuracy of Lung Ultrasound for Pulmonary Tuberculosis in out-patients from Papua New Guinea, a Resource-Limited setting

Maria Lightowler[1], Juno Min[2], Anna Nape[3], Thelma Galowa[3], *Carolyn Hemo[3], Erin Stratta[4], Matthew Fentress[5], Stefan Weber[6], Mischa Huson[7], Laura Sannino[8], Sarala Nicholas[1], Helena Huerga[1].*

[1]Epicentre, Paris, France, [2]Médecins Sans Frontières, Amsterdam, Netherlands, [3] Médecins Sans Frontières Port Moresby, Papua New Guinea, [4]Médecins Sans Frontières, New York, United States, [5] Contra Costa / University of California, San Francisco, United States, [6]University Hospital Heidelberg, Department for Infectious Disease and Tropical Medicine, [7]Erasmus Medical Center, Rotterdam, Netherlands, Médecins Sans Frontières, Paris, France. Email: maria.lightowler@brussels.msf.org

Corresponding author: Maria Lightowler E-mail: Maria.lightowler@brussels.msf.org
Address: 34 Avenue Jean Jaurès 70519. Paris, France

Highlights

- Lung ultrasound shows high sensitivity comparable to chest Xray for TB detection
- Specificity of lung ultrasound is low; no optimal findings were identified
- Study conducted in a high-burden, low-resource setting in Papua New Guinea
- Lung ultrasound may support tuberculosis diagnosis where radiography is unavailable
- Scoring system developed with good accuracy including specificity; further validation is needed

Abstract

Objective: to evaluate the diagnostic accuracy of lung ultrasound (LUS) for pulmonary tuberculosis (PTB) in Papua New Guinea.

Methods: Prospective observational study including out-patients with presumptive PTB (cough ≥2 weeks) attending a TB clinic in Port Moresby, Papua New Guinea. Participants underwent clinical assessment, GeneXpert Ultra-MTB/RIF, Chest X-ray (CXR), and LUS. Diagnostic accuracy of LUS findings was assessed using GeneXpert as reference standard. Accuracy of CXR and agreement with LUS were also evaluated. A LUS scoring system was developed using LASSO logistic regression.

Results: Between May 2022 and May 2023, 512 participants were enrolled and 488 with GeneXpert were included in the analyses. Median age was 30 [IQR 23-44] and 55% were male. GeneXpert was positive in 149 (30.5%). Combined LUS findings sensitivity was 92.6% (95%CI 90.1–95.1) and specificity 46.8% (95% CI: 42.1–51.5). CXR sensitivity was 91.3% (95% CI: 86.6–93.9) and specificity 65.1% (95% CI: 60.7–69.6). Agreement between LUS and CXR was moderate (kappa=0.48). The LUS score achieved 82.8% sensitivity and 84.2% specificity.

Conclusions: LUS demonstrates high sensitivity for detecting PTB, equivalent to CXR, but low specificity. LUS may have diagnostic value, particularly where radiography is unavailable. The scoring system that showed higher specificity should be validated in future studies.

Key words: Pulmonary Tuberculosis, Lung ultrasound, diagnostic accuracy, Papua New Guinea, Resource-Limited Settings

1. Introduction

Tuberculosis (TB) remains one of the most devastating infectious diseases globally, ranking as the leading cause of death from a single pathogen. In 2023, the World Health Organization (WHO) estimated 10.8 million new TB cases and 1.25 million TB-related deaths worldwide. Notably, only 8.2 million of these cases were officially diagnosed, underscoring a substantial gap in case detection and access to diagnostic services [1].

Papua New Guinea (PNG) bears a substantial high TB burden, including multidrug and rifampicin resistant TB (MDR/RR-TB). In 2022, PNG reported an estimated TB incidence of 424 cases per 100,000 population, one of the highest in the Western Pacific region [1]. Operational challenges in achieving bacteriological confirmation, particularly in rural and remote regions, contribute to delayed or missed diagnoses [2].

Effective TB diagnosis is essential to closing the current detection gap. Diagnostic innovations in recent years include the development of WHO-endorsed rapid molecular assays that can simultaneously detect *Mycobacterium tuberculosis* and resistance to key drugs [3]. Chest X-ray (CXR) is recommended by WHO as

screening and diagnostic tool and is particularly useful when bacteriological confirmation is lacking and in children [4]. CXR is also recommended for TB screening and has a higher sensitivity than symptom screening alone. Despite its utility, CXR deployment in high-burden, resource-limited settings is often constrained by high costs, limited infrastructure, and shortage of trained radiologists [5]. While artificial intelligence (AI)-driven software for automated CXR interpretation has been recommended by WHO for TB screening [6], its widespread implementation remains limited by cost and logistical barriers in low-resource settings [7].

Ultrasound (US) offers several advantages, including lower cost [8], safety profile and radiation-free [9], and minimal infrastructure [10]. Advances in portability, image resolution, and affordability have facilitated the use as a point-of-care modality performed directly by clinicians (i.e. point-of-care ultrasound or POCUS) [11]. US is increasingly being used to support the detection of extrapulmonary TB (EPTB) in people living with HIV (PLHIV) [12]. It aids in identifying pleural and pericardial effusions, abdominal lymphadenopathy, and lesions in the liver, spleen, and kidneys suggestive of TB [13–15] and has also shown utility in detecting mediastinal lymphadenopathy in paediatric TB [16]. Some studies have reported lung ultrasound (LUS) abnormalities in patients diagnosed with pulmonary TB (PTB) [17–19] and have proposed LUS as a potential triage tool for PTB [209].

Despite these promising findings, the evidence regarding the diagnostic accuracy of LUS for PTB remains limited and heterogeneous. A 2021 systematic review of six studies (five in adults, one in children) reported variable sensitivity using different reference standards and high risk of bias. In adults, subpleural nodules (SUNs) and lung consolidation emerged as the most sensitive findings, although specificity data

was scarce [21]. In a paediatric study from a high TB/HIV burden setting, LUS sensitivity was 64% and specificity 42.7% using CXR as the reference standard [22] and a proof-of-concept study in adults reported LUS sensitivity of 91% and specificity of 46% against bacteriological confirmation [23].

This study aims to expand the limited evidence regarding the role of LUS in TB diagnosis and its potential use as an accessible, point-of-care imaging modality, particularly when CXR is unavailable. We evaluated the diagnostic accuracy of LUS for PTB using bacteriological TB confirmation as reference standard in outpatients with presumed PTB in PNG. We also assessed the diagnostic accuracy of CXR using the same reference standard, as well as the agreement between LUS and CXR in identifying TB. Furthermore, we developed a novel diagnostic scoring system to enhance the performance of LUS for PTB diagnosis.

2. Methods

2.1. Study setting and design

This prospective observational diagnostic study was conducted in the TB clinic at the Gerehu Hospital in Port Moresby, PNG. The TB clinic is an out-patient Ministry of Health facility that has been supported by Médecins Sans Frontières (MSF) since 2016. The clinic provides diagnostic and treatment services for both drug-susceptible (DS-TB) and drug-resistant tuberculosis (DR-TB).

2.2. Study population

The study population consisted of individuals aged 10 years and older, who presented to the Gerehu TB clinic for evaluation and TB care. Inclusion criteria were: (1) presumptive PTB (defined as self-reported cough lasting two weeks or more) or clinician referral for CXR. Exclusion criteria were: (1) patients requiring inpatient management; and (2) individuals already receiving TB treatment at the time of screening. All adult participants provided written informed consent (or written informed parental consent and child assent if <18 years).

Participants were mostly enrolled consecutively among eligible patients. However, on days when the number of eligible patients exceeded US capacity, a maximum of four participants were randomly selected to maintain imaging quality.

2.3. Study procedures

All consenting participants underwent an initial clinical assessment including medical history, evaluation of TB exposure, physical examination, and sputum collection for Xpert MTB/RIF Ultra assay (Cepheid, Sunnyvale, CA, USA). All participants underwent both CXR at an accredited radiology facility and LUS conducted on site either on the same or following day by a study-trained clinician.

Ultrasound

Scanning technique

US was performed by two newly trained clinicians who completed a 10-hour introductory POCUS course led by a certified instructor, followed by a two-week, 50-hour hands-on training. Competency was demonstrated through 25 high-quality scans covering the full protocol, reviewed with feedback by the instructor followed by 25 additional scans independently reviewed remotely. After meeting these requirements,, both clinicians jointly performed all study US , each contributing approximately 50% of scans.

A portable M-Turbo ultrasound machine (Sonosite, Fujifilm) with a 6.0 to 13.0 MHz linear transducer (“Small Parts" preset, 4 cm depth) was used for initial scans. For deeper structures or study participants with a larger body habitus, a 2.0 to 5.0 mHz curvilinear transducer (abdominal preset) was used. Scans were conducted with patients in supine or seated positions (pleural effusion measurements, posterior views).

Sixteen lung zones were systematically examined (Figure 1). In each zone, longitudinal and transverse scans were performed, with at least one 10-second longitudinal video clip recorded. Pathological findings (e.g., consolidation, cavity, effusion) were documented with images and measured, and mapped to specific zones to enable separate tracking of overlapping pathologies.

Additionally, a subxiphoid view was obtained in the supine position to assess and measure for pericardial effusion, using a low-frequency probe angled cranially. Alternatively, a parasternal long-axis view (PLAX) was used. For consistency, we refer to the entire procedure (including pleural and pericardial scans) as LUS throughout this manuscript.

LUS interpretation

Pseudonymized LUS images and clips were remotely reviewed by POCUS experts (experienced researchers in TB-specific ultrasound interpretation) and findings documented in standardized electronic CRFs. Based on the combination of these findings, three non-exclusive diagnostic categories were predefined per-protocol for TB detection, one main and two alternative definitions. (Table 1; Figure 2).

Definitions were adapted from prior studies [18, 19] and refined through research expert discussions to reach consensus.

Consolidation was subcategorised as ≤ 1cm or > 1cm. To reduce variability in interpretation between SUN and small consolidations, detailed classification criteria were standardised (Supplementary table 1).

Chest X-ray

Pseudonymized DICOM CXR images were remotely interpreted by an expert radiologist (15 years of experience in TB CXR interpretation) for the presence of cavities, miliary pattern, reticulonodular infiltrates, lobar or segmental consolidation, nodular lesions, intrathoracic lymphadenopathy, pleural effusion, and an enlarged cardiac silhouette with a “water-bottle” configuration (Supplementary file, Table 2). Finding location was specified (apical, upper, or lower lung zones; right or left). Based on the combination of these findings, three non-exclusive diagnostic categories were predefined for detecting TB.

To reduce interpretation bias, all image reviewers were blinded to clinical and laboratory data including GeneXpert results and treatment decisions. The experts

interpreting the CXR and LUS were additionally blinded to the results of the other imaging modality.

To enhance consistency across LUS expert interpretations, the POCUS experts initially reviewed a common set of 20 LUS scans, discussed the findings, and aligned on study definitions prior to initiating formal image review.

2.4. Data collection and management

Clinical, laboratory and treatment data were recorded on paper-based case report forms (CRF) and secondarily on REDCAP [24]. by local study staff, overseen by the principal investigator. Remote imaging interpretation was also documented in standardized REDCap CRFs.

2.5. Study outcomes and data analyses

The primary outcome was the diagnostic accuracy of individual and a predefined combination of LUS findings for detecting TB (Main definition), assessed against the reference standard. Additionally, diagnostic accuracy was estimated using two alternative definitions for predefined combined LUS findings highly suggestive of TB. LUS was considered as not highly suggestive of TB when the findings did not fulfil the definition. Diagnostic accuracy metrics—including sensitivity, specificity, positive predictive value (PPV), and negative predictive value (NPV)—were calculated. The diagnostic accuracy of individual and predefined combined CXR findings was also evaluated using the same metrics. Additionally, the agreement between LUS and CXR

in identifying cases classified as “Highly suggestive of TB” (Main definition) was assessed using Cohen’s kappa (κ) coefficient.

The Xpert MTB/RIF Ultra assay result was used as the reference standard for TB diagnosis. Participants were classified as either having confirmed TB or non-TB based on the assay positive or negative results, respectively. Those without bacteriological confirmation but treated based on clinical assessment were categorized as 'unconfirmed TB' and were excluded from the diagnostic primary accuracy analyses.

Additionally, two secondary analyses were conducted: one including patients with unconfirmed TB and another excluding participant under 15 years of age.

Baseline demographic and clinical characteristics were presented for the entire cohort and stratified by diagnostic categories.

Mean and standard deviation (SD) were used for normally distributed numerical data, and median and inter-quartile range (IQR) for non-normally distributed data. Categorical variables were summarised as frequencies and proportions.

To explore combinations of LUS findings beyond predefined combinations with potentially increased diagnostic accuracy and develop a clinically applicable diagnostic score, we used logistic regression with least absolute shrinkage and selection operator (LR-LASSO). The dataset was randomly divided into a training set (70%) and a test set (30%). Model generalizability was optimized using k-fold cross-validation on the training set to select the most suitable tuning parameter (λ). The model was then retrained on the full training set with this λ, and the resulting coefficients were scaled into a simplified point-based score. Risk scores were generated for the test set, and an optimal cut-off was determined via ROC analysis to dichotomize PTB

status. Diagnostic metrics (sensitivity, specificity, accuracy) were derived from the resulting confusion matrix.

All estimates are reported with 95% confidence intervals (CI). Most statistical analyses were performed using Stata version 15.1 (StataCorp LLC, College Station, TX, USA). Analyses involving LR-LASSO modelling, data splitting, cross-validation, and diagnostic metric calculations were conducted in R (version 4.4.2; R Foundation for Statistical Computing, Vienna, Austria).

2.6. Ethical considerations

The study was approved by the Medical Research Advisory Committee of PNG (No. 19.01) and the MSF Ethical Review Board (ID: 1976). The study was conducted in accordance with the Declaration of Helsinki [25] and the International Ethical Guidelines for Health-Related Research Involving Humans by CIOMS [26].

3. Results

3.1 Participants' characteristics

Between May 16, 2022, and May 8, 2023, 1503 patients were screened at the Gerehu TB clinic. Of these, 512 were enrolled in the study, and 488 were tested with GeneXpert MTB/RIF and included in the analyses (Figure 2). Participants were predominantly male (270, 55.3%), and median age was 30 years [IQR: 23–44]. HIV-prevalence was 2.0%. Approximately 50% reported contact with a TB case, primarily within the household, and 21% had a history of previous TB treatment (Table 2).

The 488 participants tested with GeneXpert MTB/RIF ultra-assay, were classified as follows: 149 (30.5%) confirmed TB, 55 (11.3%) unconfirmed TB, and 284 (58.2%) as non-TB. In total, 433 participants with confirmed TB and non-TB were included in the accuracy analyses. Among the confirmed TB patients, 129 (86.6%) were classified as only pulmonary TB, and 20 (13.4%) had both pulmonary and extrapulmonary involvement. Rifampicin resistance was identified in two participants.

Among the 55 individuals excluded from the primary accuracy analyses, a higher proportion were male and slightly older compared to the included population. (Table 2)

3.2 Lung ultrasound findings

The average duration of the LUS examination performed by the trained clinician was 39 minutes (range: 20 – 69 minutes). Image quality was rated by the POCUS experts as “good” in 225 participants (46.5%), “adequate” in 246 (50.8) and "poor” in 13 (2.7%).

The most common LUS findings among participants were small consolidations < 1 cm (67%), SUNs (48%) and larger consolidations > 1 cm (46%). Less frequent findings were miliary pattern (11%), pericardial effusion (9%) and cavities (3%). All LUS findings were observed more frequently in participants with TB compared to those without TB (Table 3). Full details of LUS findings by diagnostic group are provided in the Supplementary Material (Supplementary Table 3).

Diagnostic performance varied among the different LUS findings. SUNs showed moderate accuracy, with a sensitivity of 64% and specificity of 60%. Small consolidations demonstrated higher sensitivity (79%) but lower specificity (39%),

whereas larger consolidations showed slightly lower sensitivity (76%) and moderate specificity (69%) (Table 3).

The diagnostic accuracy of SUN varied depending on the specifications of the SUN characteristics. Restricting SUN finding to a quantity of more than 5 or a size of more than 5mm, increased the specificity to 92% and 95% respectively, while decreasing the sensitivity to 20% and 21%, respectively (Table 3).

3.3 Chest X-ray findings

CXR image quality, as assessed by the expert radiologist, was rated as “good” for 153 CXR (31.4%), “adequate” for 286 (58.7%) and “poor” for 48 (9.9%).

The most common CXR findings among confirmed TB participants were reticulonodular infiltrates (70%) and cavities (23%) (Table 4). Cavities were often multiple and > 1cm (Supplementary Table 4)

CXR findings showed variable diagnostic accuracy for TB. Reticulonodular infiltrates and cavities had the highest sensitivities, 70% and 54%, respectively and lymphadenopathy and miliary pattern had the highest specificities, 97% and 100%, respectively. Other findings demonstrated lower sensitivity despite high specificity.

3.4 Diagnostic accuracy of combined imaging findings for TB detection

Using a predefined combination of imaging findings for “Highly suggestive of TB” (Main definition), LUS demonstrated a sensitivity of 92.6% (95% CI: 90.1–95.1) and specificity of 46.8% (95% CI: 42.1–51.5). The positive predictive value was 47.8% (95%CI 43.1-52.5) and the negative predictive value was 92.3% (95%CI 89.9-94.9).

CXR showed a sensitivity of 91.3% (95% CI: 86.6–93.9) and specificity of 65.1% (95% CI: 60.7–69.6) (Table 5).

Using alternative definitions for “highly suggestive of TB”, LUS sensitivity decreased, 69% and 65% using alternative definitions 1 and 2 respectively, while the specificity increased, 64% and 74%, respectively (Table 5).

Secondary analysis showed that including unconfirmed TB yielded a sensitivity of 91.7% (95% CI: 89.2–94.1; Supplementary Table 5), while excluding participants <15 years produced similar results than the primary analyses (Supplementary Table 6).

3.5 Agreement between CXR and LUS

The agreement between CXR and LUS in categorising participants as “Highly suggestive of TB” using the Main definition was moderate with a Cohen’s kappa of 0.48 (95%CI 0.40-0.56). This indicates that the two imaging modalities often identify different subsets of patients with TB. (Supplementary file, Table7).

3.6 LUS-Based Diagnostic Score

The final LR-LASSO model selected several LUS findings as predictors of PTB, which were incorporated into a point-based scoring system ranging from 0 to 6 points: miliary pattern in ≥2 lung zones (2 points), consolidation >1 cm in apical or upper zones (2 points), pleural effusion (1 point), and SUN or consolidation ≤1 cm in the apical zone (1 point) (Supplementary file, Table8). Using a threshold of 1.5, individuals with scores of 2 or higher were classified as PTB positive. The score demonstrated a sensitivity of 82.8% (95% CI: 64.2–94.2) and a specificity of 84.2% (95% CI: 72.1–92.5) (Supplementary file, Table 9and Figure 1).

4. Discussion

This study provides evidence regarding the potential of LUS as a diagnostic tool for pulmonary TB in outpatients aged over 10 years, particularly in settings without access to CXR. Our findings suggest that LUS has high sensitivity and low specificity for PTB. The LUS has a comparable sensitivity to that of CXR but lower specificity. Both modalities have similar performance in ruling out PTB.

Study findings

Our study findings align with previous studies. A proof-of-concept study in South Africa reported 85% sensitivity and 52% specificity for LUS in detecting thoracic abnormalities (consolidation, subpleural pathology, cavity, any B-patterns, pleural line irregularities, or pleural effusion) using bacteriologically confirmed TB as the reference standard [22]. Montuori et al. found a sensitivity of 86% and specificity of 63% using a combination of subpleural nodules and apical consolidation, though 14% of TB cases lacked bacteriological confirmation [18]. The slightly higher specificity reported in studies by Montuori et al. [18] and Fentress et al. [22] may be influenced by differences in how LUS findings were defined and applied. They may have applied stricter criteria for lesion size, location, or pattern recognition, which could reduce false positives. Additionally, differences in real-time image acquisition versus interpretation from recorded clips, as well as variations in study populations, may also contribute to these discrepancies.

Importantly, the most frequent LUS findings present in confirmed TB cases were consolidations ≤1 cm (78.5%), consolidations >1 cm (75.2%), and SUNs (63.8%). Findings with the highest specificity were SUNs >5 mm (95.4%), SUNs located in the

apical zones (88%), and pericardial effusion (93.7%). These results align with previous studies, such as Montuori et al. [32], which reported a specificity of 66.7% for SUN, and Fentress [22]. Cavities were rarely detected in our study, corroborating known limitations of LUS in identifying cavitations [26].

Most of our lung imaging was performed using a linear probe with 4 cm starting depth, likely improving detection of subtle findings, such as small SUNs compared to a curvilinear probe on an abdominal preset. This approach may have increased sensitivity but reduced specificity.

We developed a LR-LASSO derived 6-points scoring model incorporating key LUS findings—miliary pattern in at least 2 lung zones, consolidation > 1 cm in the apical or upper lung zone, pleural effusion, and either SUN or small consolidations (≤1 cm) in the apical lung zone. At a threshold of 2 points, the model showed good diagnostic performance of the score (sensitivity 82.8%, specificity 84.2%). The scoring-model simplifies interpretation by grouping together SUN and small consolidations, which are intrinsically difficult to differentiate. It also streamlines image acquisition by excluding pericardial effusion. These advantages may further facilitate the implementation use of LUS in resource-limited settings.

Training non-specialist clinicians to perform LUS using a standardized acquisition protocol was successful, with Health Extension Officers consistently obtaining high-quality ultrasound images. This aligns with evidence from the Focused Assessment with Sonography for HIV-associated TB (FASH) protocol, which demonstrated that novice clinicians can be trained not only to acquire but also to interpret sonographic findings for extrapulmonary TB [26]. Unlike other POCUS modules that are typically

performed and interpreted immediately by performing clinicians, our study focused solely on image acquisition, with expert reviewers interpreting LUS exams remotely. However, the time required for LUS image acquisition followed by external interpretation may limit practical implementation of this approach in busy clinical settings. Nevertheless, this time is expected to be reduced following the training and implementation phase.

Strengths and limitations

The strengths of this study include the use of a robust reference standard (bacteriologically confirmed TB), a large outpatient sample that addresses limitations of previous studies [20], and a standardized image acquisition protocol Importantly, we report both sensitivity and specificity for individual and combined imaging findings, and diagnostic accuracy estimates remained consistent when including patients with unconfirmed TB, reinforcing our primary results. LUS and CXR images were interpreted by blinded experts, minimizing the risk of bias. Furthermore, LUS acquisition by trained clinicians on site supports the applicability of our results to real-world, low-resource settings.

Our study has also limitations. It was conducted in a high TB burden setting, where lung sequelae from previous TB may have affected image interpretation. Therefore, generalizability to low-burden TB settings may be limited. Inter-reader interpretation variability may have occurred, as four POCUS experts reviewed subsets of US examinations. Ideally, each exam would have been reviewed by multiple readers, but this was not possible due to time constraints and expert reviewer availability. Additionally, sub-centimetre findings such as subpleural nodules are difficult to identify

and distinguish on recorded clips without hands-on manipulation of the ultrasound transducer and real-time evaluation of the images. Operator dependency remains a notable limitation of ultrasound in general [28, 29]. Although image acquisition was relatively standardized, interpretation is prone to inter-reader variability and subjectivity. This is particularly relevant when distinguishing SUN from small consolidations, which often share overlapping features. Despite efforts to apply consistent distinguishing criteria, a degree of subjectivity remains. Similarly, differentiating cavities from consolidation remains difficult; however, given the rarity of cavities in our dataset, this had minimal practical impact on our results. Emerging artificial intelligence (AI) solutions have potential to increase objectivity and reduce inter-reader variability. Deep-learning approaches are showing promise in automating US image interpretation and improving diagnostic accuracy [30]. Specific analysis in age subgroups, particularly those under 15 years—who more frequently present with extrapulmonary TB and lymph node involvement [31]—was not possible due to the small sample size in this group. While the model-derived scoring system showed promising results, prospective validation will be required to assess its diagnostic value.

5. Conclusions

In summary, LUS demonstrates a high sensitivity for PTB, equivalent to CXR, although the specificity is low. LUS may have potential for PTB diagnosis as an imaging modality, particularly when CXR is unavailable. We did not identify a combination of LUS findings providing an optimal balance of sensitivity and specificity for PTB diagnosis. However, our diagnostic scoring system offers a pragmatic alternative, with notably higher specificity. Future studies are needed to externally validate the

proposed score and to explore whether integrating the FASH protocol for extra-pulmonary TB, enhance diagnostic yield.

6. Acknowledgments

We thank all study participants, and the Gerehu study team, specially Anna Nape for the study coordination and Carolyn Hemo for performing the ultrasounds, study Community Health worker health extension officers, laboratory technicians, data supervisors (Ibrahim Seyni Am) a as well as the entire Médecins Sans Frontières team in Port Moresby for supporting the preparation and implementation phase of the study, including MSF field project coordinator, mission epidemiologist, medical coordinator and cell medical responsible

Conflicts of interest

The authors declare no competing interests.

Ethical approval

The study was approved by the Medical Research Advisory Committee of Papua New Guinea (No. 19.01) and the Medecins Sans Frontieres Ethical Review Board (ID: 1976).

Funding source

This work was funded by Médecins Sans Frontières – Operational Center Paris.

Supplementary materials

Supplementary material associated with this article can be found, in the online version,

07. References

[1] World Health Organization. Global tuberculosis report 2024. Geneva: World Health Organization; 2024. Available from: https://iris.who.int/bitstream/handle/10665/379339/9789240101531-eng.pdf?sequence=1

[2] Bita S, Kelebi T, Holmes A, Vaccher S, Majumdar SS, Greig J. TB burden and diagnostic challenges at Sandaun Provincial Hospital in West Sepik Province of PNG, 2016–2021. Public Health Action. 2024. http://dx.doi.org/10.5588/pha.24.0016

[3] World Health Organization. WHO consolidated guidelines on tuberculosis. Module 3: diagnosis – rapid diagnostics for tuberculosis detection. 3rd ed. Geneva: World Health Organization; 2024.

[4] World Health Organization. Chest radiography in tuberculosis detection. Geneva: World Health Organization; 2016.

[5] Pomykala K, Desai I, Jardon M, et al. Imaging of tuberculosis in resource-limited settings. Curr Radiol Rep. 2019;7:23. https://doi.org/10.1007/s40134-019-0335-7

[6] Use of computer-aided detection software for tuberculosis screening: WHO policy statement. Geneva: World Health Organization; 2025. (License: CC BY-NC-SA 3.0 IGO). Cataloguing-in-Publication (CIP) data available at: https://iris.who.int/[7] Qin ZZ, Naheyan T, Ruhwald M, Denkinger CM, Gelaw S, Nash M, et al. A new resource on artificial intelligence powered computer automated detection software products for tuberculosis programmes and implementers. Tuberculosis (Edinb). 2021;127:102049. https://doi.org/10.1016/j.tube.2020.102049 PMID: 33440315

[8] Parker L, Nazarian LN, Carrino JA, Morrison WB, Grimaldi G, Frangos AJ, et al. Musculoskeletal imaging: Medicare use, costs, and potential for cost substitution. J Am Coll Radiol. 2008;5(3):182–8.

[9] Smith-Bindman R, Aubin C, Bailitz J, Bengiamin RN, Camargo CA, Corbo J, et al. Ultrasonography versus computed tomography for suspected nephrolithiasis. N Engl J Med. 2014;371(12):1100–10.

[10] Lichtenstein D, Goldstein I, Mourgeon E, Cluzel P, Grenier P, Rouby JJ. Comparative diagnostic performances of auscultation, chest radiography, and lung ultrasonography in acute respiratory distress syndrome. Anesthesiology. 2004;100:9–15. https://doi.org/10.1097/00000542-200401000-00006

[10] Sorensen B, Hunskaar S. Point-of-care ultrasound in primary care: a systematic review of generalist performed point-of-care ultrasound in unselected populations. Ultrasound J. 2019;11(1):31. https://doi.org/10.1186/s13089-019-0145-4 PMID: 31749019

[12] Bobbio F, Di Gennaro F, Marotta C, et al. Focused ultrasound to diagnose HIV-associated tuberculosis (FASH) in the extremely resource-limited setting of South Sudan: a cross-sectional study. BMJ Open. 2019;9:e027179. https://doi.org/10.1136/bmjopen-2018-027179

[13] Goblirsch S, Bahlas S, Ahmed M, Brunetti E, Wallrauch C, Heller T. Ultrasound findings in cases of extrapulmonary TB in patients with HIV infection in Jeddah, Saudi Arabia. Asian Pac J Trop Dis. 2014;4(1):14–7.

[14] Griesel R, Cohen K, Mendelson M, Maartens G. Abdominal ultrasound for the diagnosis of tuberculosis among human immunodeficiency virus-positive inpatients with World Health Organization danger signs. Open Forum Infect Dis. 2019;6(4):ofz094. https://doi.org/10.1093/ofid/ofz094

[15] Kahn D, Pool KL, Phiri L, Chibwana F, Schwab K, Longwe BA, et al. Diagnostic utility and impact on clinical decision making of focused assessment with sonography for HIV-associated tuberculosis in Malawi: a prospective cohort study. Glob Health Sci Pract. 2020;8(1):28–37. https://doi.org/10.9745/GHSP-D-19-00251

[16] Pool KL, Heuvelings CC, Bélard S, Grobusch MP, Zar HJ, Bulas D, et al. Technical aspects of mediastinal ultrasound for pediatric pulmonary tuberculosis. Pediatr Radiol. 2017;47(13):1839–48.

[17] Babasa III R, Bithao P. Diagnostic accuracy of point-of-care lung ultrasound among patients suspected of having pulmonary tuberculosis. 2019.

[18] Agostinis P, Copetti R, Lapini L, Badona Monteiro G, N'Deque A, Baritussio A. Chest ultrasound findings in pulmonary tuberculosis. Trop Doct. 2017;47(4):320–8. https://doi.org/10.1177/0049475517709633 PMID: 28541140

[19] Montuori M, Casella F, Casazza G, Franzetti F, Pini P, Invernizzi C, et al. Lung ultrasonography in pulmonary tuberculosis: a pilot study on diagnostic accuracy in a high-risk population. Eur J Intern Med. 2019;66:29–34.

[20] Nathavitharana RR, Garcia-Basteiro AL, Ruhwald M, Cobelens F, Theron G. Reimagining the status quo: how close are we to rapid sputum-free tuberculosis diagnostics for all? EBioMedicine. 2022;78.

[21] Bigio J, Kohli M, Klinton JS, MacLean E, Gore G, Small PM, et al. Diagnostic accuracy of point-of-care ultrasound for pulmonary tuberculosis: a systematic review. PLoS One. 2021;16(5):e0251236. https://doi.org/10.1371/journal.pone.0251236 PMID: 33961639

[22] Erem G, Otike C, Okuja M, et al. Diagnostic accuracy of chest ultrasound scan in the diagnosis of childhood tuberculosis. PLoS One. 2023;18(9):e0287621.

[23] Fentress M, Henwood PC, Maharaj P, et al. High sensitivity of ultrasound for the diagnosis of tuberculosis in adults in South Africa: a proof-of-concept study. PLOS Glob Public Health. 2022;2:e0000800.

[24] Harris PA, Taylor R, Minor BL, Elliott V, Fernandez M, O'Neal L, et al. The REDCap consortium: building an international community of software platform partners. J Biomed Inform. 2019;95:103208. https://doi.org/10.1016/j.jbi.2019.103208

[25] World Medical Association. Declaration of Helsinki: ethical principles for medical research involving human participants. JAMA. 2024;333(1):71–74.

[26] Council for International Organizations of Medical Sciences (CIOMS), World Health Organization. International ethical guidelines for health-related research involving humans. 4th ed. Geneva: CIOMS; 2016.

[27] Heller T, Wallrauch C, Lessells RJ, Goblirsch S, Brunetti E. Short course for focused assessment with sonography for HIV associated tuberculosis: preliminary results in a rural South African hospital. Am J Trop Med Hyg. 2010;82(3):512–5.

[28] Suttels V, Du Toit JD, Fiogbé AA, Wachinou AP, Guendehou B, Alovokpinhou F, et al. Point-of-care ultrasound for tuberculosis management in Sub-Saharan Africa—a balanced SWOT analysis. Int J Infect Dis. 2022;123:46–51. https://doi.org/10.1016/j.ijid.2022.07.009 PMID: 35811083

[29] Conlon TW, Yousef N, Mayordomo-Colunga J, Tissot C, Fraga MV, Bhombal S, et al. Establishing a risk assessment framework for point-of-care ultrasound. Eur J Pediatr. 2022;181(4):1449–57. https://doi.org/10.1007/s00431-021-04324-4 PMID: 34846557

[30] Shen YT, Chen L, Yue WW, Xu HX. Artificial intelligence in ultrasound. Eur J Radiol. 2021;139:109717.

[31] Dubois MM, Brooks MB, Malik AA, Siddiqui S, Ahmed JF, Jaswal M, Amanullah F, Becerra MC, Hussain H. Age-specific clinical presentation and risk factors for extrapulmonary tuberculosis disease in children. *Pediatr Infect Dis J*. 2022 Aug;41(8):620–625. doi:10.1097/INF.0000000000003584. PMID: 35849791; PMCID: PMC9281512.

Diagnostic Accuracy of Lung Ultrasound for Pulmonary Tuberculosis in out-patients from Papua New Guinea, a Resource-Limited setting

Figures

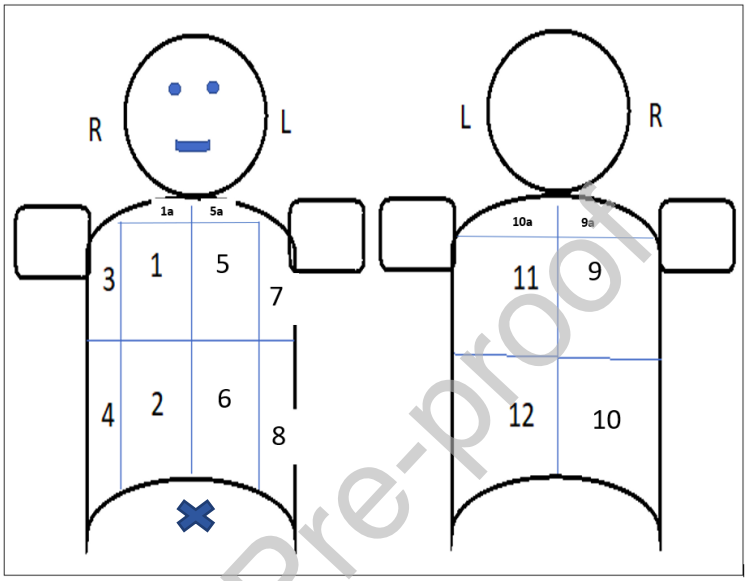

Figure 1. Lung zones and apical sweep zones (16 zones): anterior (mid-clavicular), lateral (mid-axillary), and posterior (mid-scapular) zones on both sides, each divided into upper and lower zones, plus bilateral apical sweeps. Scanning began in the supine position (zones 1–8), followed by seated posterior views (zones 9–16)

• Right anterior mid-clavicular line -- apical: 1a • Right anterior mid-clavicular line – upper: 1 • Right anterior mid-clavicular line – lower: 2 • Right mid-axillary line -- upper: 3 • Right mid-axillary line -- lower: 4 • Right posterior mid-scapular line -- apical: 9a • Right posterior mid-scapular line – upper: 9 • Right posterior mid-scapular line -- lower: 10 • X → Subxiphoid view	• Left anterior mid-clavicular line -- apical: 5a • Left anterior mid-clavicular line -- upper: 5 • Left anterior mid-clavicular line – lower: 6 • Left mid-axillary line -- upper: 7 • Left mid-axillary line -- lower: 8 • Left posterior mid-scapular line -- apical: 11a • Left posterior mid-scapular line – upper: 11 • Left posterior mid-scapular line -- lower: 12

Fig 2 A	Fig 2 B	Fig 2 C
Fig 2 D	Fig 2 E	Fig 2 F

Figure 2. Typical thoracic ultrasound findings in tuberculosis. A, Subpleural nodule: Subpleural round hypoechoic nodule measuring less than 1 cm and demonstrating posterior acoustic enhancement. B, Consolidation: Hypoechoic area within lung parenchyma. C, Cavity: Hypoechoic area with ill-defined margins and an avascular center (no flow on colour Doppler). D, Miliary pattern: Subpleural granular appearance with diffuse B-lines that appear to emanate from the subpleural granules. E, Pleural effusion: anechoic fluid collection in the pleural space. F, Pericardial effusion: anechoic fluid surrounding the heart. *This image is used for illustration purposes only and should not be reproduced by others.*

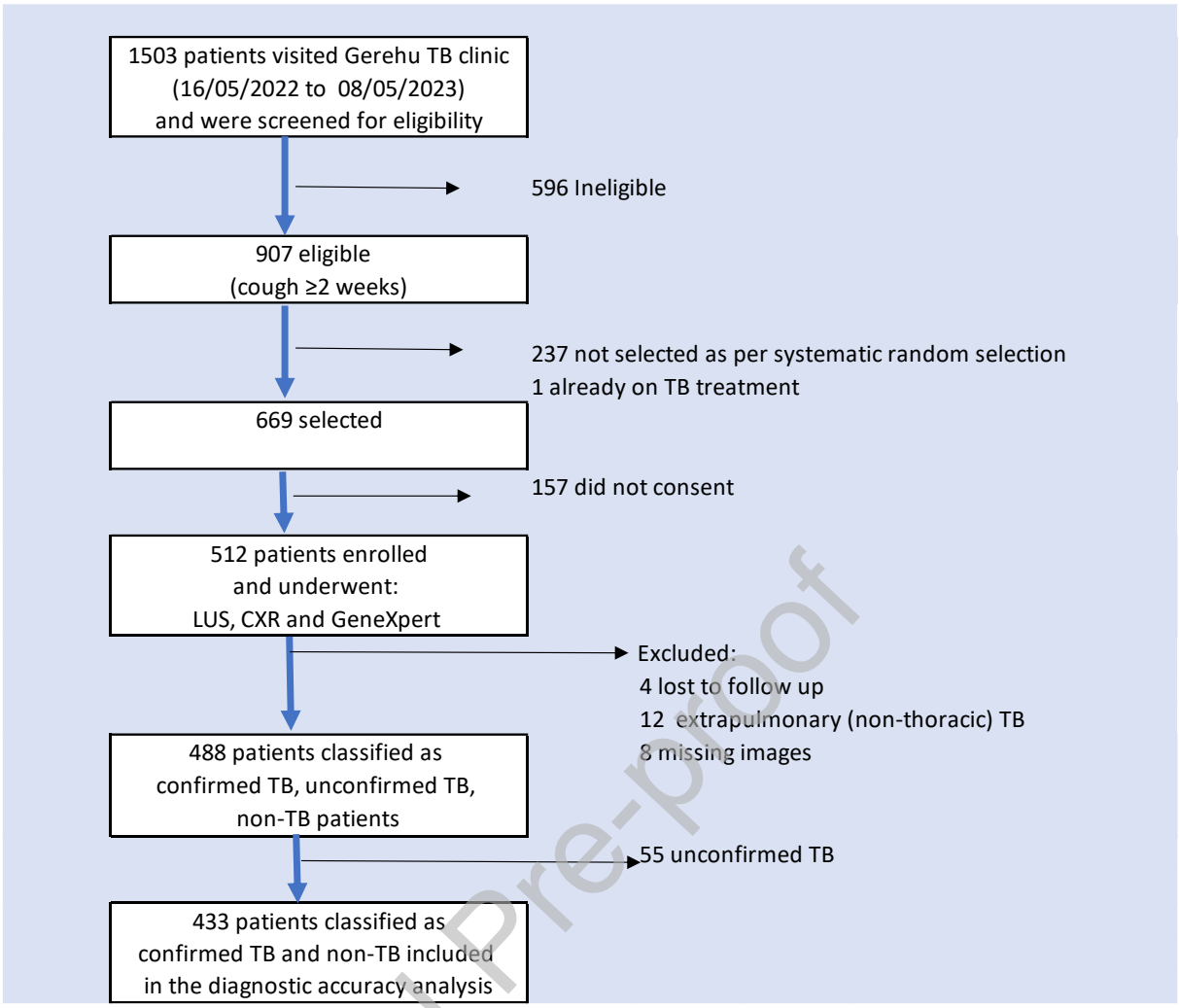

Figure 3. Study flowchart.

Diagnostic Accuracy of Lung Ultrasound for Pulmonary Tuberculosis in out-patients from Papua New Guinea, a Resource-Limited setting

Tables

	DEFINITION
Individual ultrasound findings	
Subpleural nodule (SUN)	• Well-defined, round or oval nodule immediately beneath the pleura • Vertical diameter < 1 cm (measured from the pleural line) • Hypoechoic interior with no internal echoes • Clear hyperechoic posterior wall • Posterior acoustic enhancement
Consolidation	• Hypoechoic area within lung parenchyma • Ill-defined margins with irregular, ragged posterior border ○ Speckled internal appearance, possibly with hyperechoic punctate or linear foci (air bronchograms) • Posterior acoustic enhancement inconsistent
Cavity	• Consolidation containing a central hypoechoic, avascular area (no flow on colour Doppler)
Miliary pattern	• Diffuse subpleural granular appearance with multiple B-lines originating from subpleural granules in at least one lung zone
Pleural effusion	• Fluid in the pleural space (between the parietal and visceral pleura) • Measured > 0.5 cm in depth (the diaphragm to lung) in seated position if feasible. • **Simple effusion**: entirely anechoic and free flowing • **Complex effusion**: contains echogenic debris (e.g. fibrin strands) or is loculated and not entirely anechoic

Pericardial effusion	• Fluid in the pericardial space, measured > 0.3 cm between the right ventricle and parietal pericardium.
	  ○ **Simple effusion:** s entirely anechoic
	  ○ **Complex effusion** contains echogenic material or is loculated, not free flowing

Pre-defined combination of Ultrasound findings for detecting TB	
Highly suggestive of TB (Main definition)	• Presence of any of the following findings on US —SUN in ≥2 zones (with at least one in the apical or upper zone), consolidation > 1 cm in any region, miliary pattern, cavity, pleural effusion or pericardial effusion >1 cm.
Highly suggestive (Alternative definition 1)	• SUN in ≥2 zones (with at least one in the apical zone), consolidation >1 cm in apical region, miliary pattern, cavity or pericardial effusion >1 cm

Highly suggestive (Alternative definition 2)	• SUN in ≥ 2 zones (with at least one in the apical or upper zone), consolidation > 1 cm in apical region; miliary pattern, cavity or pericardial effusion > 1 cm.
Pre-defined combination of Chest X-ray findings for detecting TB	
Highly suggestive of TB (Main definition)	• Presence of any of the following findings on CXR — reticulonodular infiltrates in any lung zone, lobar or segmental consolidation, nodular lesion, intrathoracic lymphadenopathy, pleural effusion, or an enlarged cardiac silhouette with a 'water-bottle' configuration.
Highly suggestive (Alternative definition 1)	• Presence of reticulonodular infiltrates in any lung zone, cavities, or a miliary pattern.
Highly suggestive (Alternative definition 2)	• Presence of reticulonodular infiltrates localized to the apical or upper lung zones, cavities or a miliary pattern

Table 1. Definitions of individual ultrasound findings and pre-defined combination of Ultrasound and Chest x-ray findings for detecting TB

	Non-TB (284)		**Confirmed TB (149)**		**Unconfirmed TB (55)**		**Total (488)**	
	n	**(%)**	**n**	**(%)**	**n**	**(%)**	**n**	**(%)**
Gender								
Female	141	(49.6)	57	(38.3)	20	(36.4)	**218**	**(44.7)**
Male	143	(50.4)	92	(61.7)	35	(63.6)	**270**	**(55.3)**
Age, median [IQR]	30.5	[23–44]	26	[22–36]	34	[26–43]	**30**	**[23–41]**
Age group categories (years)								
10 to ≤11	8	(2.8)	1	(0.7)	0	(0.0)	**9**	**(1.8)**
12 to ≤14	8	(2.8)	3	(2.0)	2	(3.6)	**13**	**(2.7)**
15 to ≤20	33	(11.6)	24	(16.1)	7	(12.7)	**64**	**(13.1)**
21 to ≤30	93	(32.7)	66	(44.3)	14	(25.5)	**173**	**(35.5)**
31 to ≤40	61	(21.5)	27	(18.1)	15	(27.3)	**103**	**(21.1)**
>40	81	(28.5)	28	(18.8)	17	(30.9)	**126**	**(25.8)**
Known TB contact	141	(49.8)	80	(53.7)	27	(49.1)	**248**	**(50.9)**
Household TB contact	128	(92.1)	71	(88.8)	26	(96.3)	**225**	**(91.5)**
Past Tuberculosis treatment	71	(25)	20	(13.4)	11	(20)	**102**	**(20.9)**
Previous treatment outcome (n=102)								
Cured or completed	42	(59.1)	11	(57.9)	4	(36.4)	**57**	**(56.5)**
Interrupted or failure	4	(5.6)	1	(5.3)	1	(9.1)	**6**	**(5.9)**
Unknown	25	(35.3)	8	(36.8)	6	(54.5)	**38**	**(37.6)**
Cough	289	(100)	149	(100)	55	(100)	**496**	**(100)**
Production of sputum	253	(89.1)	131	(87.9)	50	(90.9)	**434**	**(88.9)**
Weight loss	242	(85.2)	145	(97.3)	49	(89.1)	**436**	**(89.3)**
Weakness	240	(84.5)	129	(86.6)	51	(92.7)	**420**	**(86.1)**
Fever	194	(68.3)	123	(82.6)	46	(83.6)	**363**	**(74.4)**
Difficulty to breath	195	(68.7)	115	(77.2)	50	(90.9)	**360**	**(73.8)**
Night sweats	193	(68)	121	(81.2)	42	(76.4)	**356**	**(73)**

Chest pain	194	(68.3)	114	(76.5)	47	(85.5)	**355**	**(72.7)**
Loss of appetite	139	(49.1)	92	(61.7)	40	(72.7)	**271**	**(55.6)**
Other symptoms	58	(20.9)	37	(25.2)	16	(29.6)	**111**	**(23.2)**
Haemoptysis	63	(22.2)	34	(22.8)	9	(16.4)	**106**	**(21.7)**
Lymph nodes	57	(20.1)	47	(31.5)	13	(23.6)	**117**	**(24)**
Cervical/supraclavicular	46	(80.7)	45	(95.7)	11	(84.6)	**102**	**(87.2)**
Other	11	(19.3)	2	(4.2)	2	(15.4)	**15**	**(12.8)**
Ascites	4	(1.4)	2	(1.3)	6	(10.9)	**12**	**(2.5)**
Other signs	11	(4.0)	7	(4.7)	0	(0.0)	**18**	**(3.7)**
Diabetes	2	(0.7)	2	(1.3)	1	(1.8)	**5**	**(1)**
HIV status								
Positive	5	(1.8)	1	(0.7)	2	(3.6)	**8**	**(1.6)**
Negative	6	(2.1)	9	(6.1)	2	(3.6)	**17**	**(3.5)**
Unknown	271	(96.1)	138	(93.2)	51	(92.7)	**460**	**(94.8)**
Place of residency								
Northwest province resident	192	(67.6)	89	(59.7)	36	(65.5)	**317**	**(65.0)**
Northwest province suburb								
Gerehu	100	(52.1)	51	(57.3)	19	(52.8)	**170**	**(53.6)**
Oher suburbs	92	(47.9)	38	(42.7)	17	(47.2)	**147**	**(46.4)**

Table 2. Demographic and clinical characteristics at baseline, stratified by TB diagnosis (N = 488)

Ultrasound finding	Non-TB (N=284)		Confirmed TB (N=149)		Total (N=433)		Sensitivity	Specificity	PPV	NPV
	n	%	n	%	n	%	(95% IC)	(95% IC)	(95% IC)	(95% IC)
Subpleural Nodules (SUN)	113	39.8	95	63.8	**208**	**48**	63.8 (59.2–68.3)	60.2 (55.6–64.8)	45.7 (41.0–50.4)	76.0 (72.0–80.0)
Consolidation ≤1 cm	174	61.3	117	78.5	**291**	**67.2**	78.5 (74.6–82.4)	38.7 (34.1–43.3)	40.2 (35.6–44.8)	77.5 (73.5–81.4)
Consolidation >1 cm	89	31.3	112	75.2	**201**	**46.4**	75.7 (71.6–79.7)	68.7 (64.3–73.0)	55.7 (51.0–60.4)	84.4 (81.0–87.8)
Cavity	4	1.4	9	6.0	**13**	**3.0**	6.0 (3.8–8.3)	98.6 (97.5–99.7)	69.2 (64.9–73.6)	66.7 (62.2–71.1)

Miliary pattern	17	6.0	29	19.5	**46**	**10.6**	19.5 (15.7–23.2)	94.0 (91.8–96.3)	63.0 (58.5–67.6)	69.0 (64.6–73.4)
Pleural effusion	39	13.7	60	40.3	**99**	**22.9**	40.5 (35.9–45.1)	86.3 (83.0–89.5)	60.6 (56.0–65.2)	73.6 (69.4–77.7)
Pericardial effusion	18	6.3	19	12.8	**37**	**8.5**	12.7 (9.6–16.0)	93.7 (91.4–96.0)	51.4 (46.6–56.1)	67.2 (62.8–71.6)
SUN quantity >5[a]	24	8.5	29	19.5	**53**	**12.2**	19.5 (15.7–23.2)	91.6 (89.0–94.2)	54.7 (50.0–59.4)	68.4 (64.0–72.8)
SUN Size >5 mm	13	4.6	31	20.8	**44**	**10.2**	20.8 (17.0–24.6)	95.4 (93.5–97.4)	70.5 (66.2–74.8)	69.7 (65.3–74.0)
SUN in Apical	34	12	49	32.9	**83**	**19.2**	32.9 (28.5–37.3)	88.0 (85.0–91.1)	59.0 (54.4–63.7)	71.4 (67.2–75.7)
SUN Apical or upper	99	34.9	83	55.7	**182**	**42**	55.7 (51.0–60.4)	65.1 (60.7–69.6)	45.6 (40.9–50.3)	73.7 (69.6–77.9)
SUN At least in 2 zones	77	27.1	60	40.3	**137**	**31.6**	40.3 (35.7–44.9)	72.9 (68.7–77.1)	43.8 (39.1–48.5)	69.9 (65.6–74.3)

a "quantity >5" refers to the total number of SUNs observed across all lung zones

Table 2 . Distribution of lung ultrasound findings among non-TB (n=284) and confirmed TB (n=149) participants and diagnostic accuracy measures (sensitivity, specificity, PPV, NPV) (N=433)

	Non-TB (N=284)		**Confirmed TB (N=149)**		**Total (N=433)**		**Sensitivity**	**Specificity**	**PPV**	**NPV**
CXR findings	**n**	**(%)**	**n**	**(%)**	**n**	**(%)**	**(95% CI)**	**(95% CI)**	**(95% CI)**	**(95% CI)**
Reticulonodular infiltrates	60	21.1	104	69.8	**164**	**37.9**	69.8 (65.5–74.1)	78.9 (75.0–82.7)	63.4 (58.9–68.0)	83.3 (79.8–86.8)
	9	3.2	13	8.7	**22**	**5.1**	8.7	96.8	59.1	66.9

Lobar or segmental consolidation							(6.1–	11.4)	(95.1–	98.5)	(54.5–	63.7)	(54.5–	63.7)
Cavity	17	6	81	54.4	**98**	**22.6**	54.4 (49.7	59.1)	94 (91.8–	96.3)	82.7 (79.1–	86.2)	79.7 (75.9–	83.5)
Nodular lesion	25	8.8	15	10.1	**40**	**9.2**	10.1 (7.2–	12.9)	91.2 (88.5–	93.8)	37.5 (32.9–	42.1)	65.9 (61.4–	70.4)
Miliary pattern	0	0	8	5.4	**8**	**1.8**	5.3 (3.3–	7.5)	100 (100.0–	100.0)	100 (100.0–	100.0)	66.8 (62.4–	71.3)
Pleural effusion	22	7.7	41	27.5	**63**	**14.5**	27.5 (23.3–	31.7)	92.3 (89.7–	94.8)	65.1 (60.6–	69.6)	70.8 (66.5–	75.1)
Lymphadenopathy	8	2.8	22	14.8	**30**	**6.9**	14.8 (11.4–	18.1)	97.2 (95.6–	98.7)	73.3 (69.2–	77.5)	68.5 (69.2–	77.5)
Enlarged cardiac silhouette	22	7.7	5	3.4	**27**	**6.2**	3.4 (1.7–	5.1)	92.3 (89.7–	94.8)	18.5 14.9–	22.2)	64.5 (60.0–	69.0)
Apical pleural thickening	21	7.4	18	12.1	**39**	**9**	12.1 (9.0–	15.2	92.6 (90.1–	95.1)	46.2 (41.5–	50.9)	66.8 (62.3–	71.2)
Fibrosis / scarring	24	8.5	10	6.7	**34**	**7.9**	6.7 (4.3–	9.1)	91.6 (89.3–	94.2)	29.4 (25.1–	33.7)	65.2 (60.7–	69.7)

Table 3. Distribution of Chest X ray findings among non-TB (n=284) and confirmed TB (n=149) participants and diagnostic accuracy measures (sensitivity, specificity, PPV, NPV) (N=433)

	Sensitivity (95% CI)	**Specificity (95% CI)**	**PPV (95% CI)**	**NPV (95% CI)**
Main definition				
LUS[a]	**92.6** (90.1– 95.1)	46.8 (42.1– 51.5)	47.8 (43.1– 52.5)	**92.3** (89.9– 94.9)

CXR [b]	**91.3**	(88.6– | 93.9)	65.1	(60.7– | 69.6)	57.9	(53.2– | 62.5)	**93.4**	(91.1– | 95.8)
Alternative definitions												
LUS Definition 1[c]	69.1	(64.8– | 73.5)	63.7	(59.2 – | 68.3)	50.0	(45.3– | 54.7)	79.7	(76.0 – | 83.5)
LUS Definition 2 [d]	65.1	(60.6 – | 69.5)	74.3	(70.2 – | 78.4)	57.1	(52.4– | 61.7)	80.2	(76.5– | 84.0)
CXR Definition 1[e]	74.5	(70.4– | 78.6)	77.5	(73.5– | 81.4)	63.4	(58.9– | 68.0)	85.3	(81.9– | 88.6)
CXR Definition 2[f]	71.1	(66.9– | 75.4)	88.0	(85.0– | 91.1)	75.7	(71.7– | 79.8)	85.3	(82.05– | 88.7)

[a] Highly suggestive of TB (LUS Main definition): Presence of SUN in ≥2 zones (with at least one in the apical or upper), consolidation > 1 cm, a miliary pattern, cavities, pleural effusion or pericardial effusion >1 cm. Not suggestive of TB: all others.

[b] Highly suggestive of TB (CXR Main definition): Presence of reticulonodular infiltrates in any lung region, lobar or segmental consolidation, nodular lesions, lymphadenopathy, pleural effusion, or an enlarged cardiac silhouette with a 'water-bottle' shape. Not suggestive of TB: all others.

[c] Highly suggestive of TB: Presence of SUN in ≥2 zones (with at least one in the apical region), consolidation >1 cm, a miliary pattern or cavities or pericardial effusion >1 cm. Not suggestive of TB: all others.

[d] Highly suggestive of TB: Presence of SUN in ≥2 zones (with at least one in the apical or upper), consolidation > 1 cm; a miliary pattern or cavities or pericardial effusion > 1 cm. Not suggestive of TB: all others.

[e] Highly suggestive of TB: Presence of reticulonodular infiltrates in any lung zone, cavities, or a miliary pattern. Not suggestive of TB: all others.

[f] Highly suggestive of TB: Presence of reticulonodular infiltrates localized to the apical or upper lung zones, cavities or a miliary pattern. Not suggestive of TB: all others.

Table 4. Diagnostic Accuracy of Lung Ultrasound (LUS) and Chest X-Ray (CXR) for tuberculosis diagnosis: Sensitivity, Specificity, Positive Predictive Value (PPV), and Negative Predictive Value (NPV) using Main and alternative definitions

Declaration of Interest Statement

☒ The authors declare that they have no known competing financial interests or personal relationships that could have appeared to influence the work reported in this paper.

☐ The author is an Editorial Board Member/Editor-in-Chief/Associate Editor/Guest Editor for this journal and was not involved in the editorial review or the decision to publish this article.

☐ The authors declare the following financial interests/personal relationships which may be considered as potential competing interests:

Maria Lightowler on behalf of all authors